AIAA Guidance, Navigation and Control Conference and Exhibit
20 - 23 August 2007, Hilton Head, South Carolina

AIAA 2007-6855

Evaluation of GNC Strategies for Terminal Descent on Solar System Bodies

Fabrizio Reali* and Giovanni B. Palmerini‡
"Sapienza" Università di Roma, Rome, Italy

[Abstract] Due to the increasing vehicle miniaturization and to the obvious requirements for autonomy, the descent on extra terrestrial bodies poses serious concerns with respect to the accuracy and the robustness of the guidance function. Closed loop guidance will depend on the accuracy on the knowledge of the kinematic state. The paper investigates the behavior of different estimators applied to two classes of trajectories, namely a gravity turn - introduced before as an open and then as a closed-loop configuration, and a path shaped descent. All investigations have been referred to quite simple sensors' architectures, providing only altitude or slant-range measurements. Numerical simulations are provided for the atmosphere-less lunar case, as well as for the descents on Mars and Titan, where the air drag is present.

Nomenclature

g	=	gravity acceleration
h	=	altitude above the planetary body surface
n	=	thrust-to-weight ratio
r	=	down-range coordinate
t	=	time
v	=	descending probe velocity
α	=	angle between the local vertical and the thrust vector
ψ	=	angle between the local vertical and the velocity (complement to the flight path angle)

I. Introduction

DUE to mass limitation at launch, space exploration is usually exploited by means of small probes. This trend is expected to be confirmed in the near future, also based on the performances improvement obtained thanks to electronics' miniaturization, so that no reduction in performances should be allowed as a trade-off with global mass reduction. In the specific field of vehicles intended to land to solar system bodies, small probes impose serious constraints on the actuators to drive the descent, and therefore more efficient guidance strategies. The quest for simpler architectures include the sensors, so that the interest for resource-limited but performing architectures for the loop is clear. The requirement of autonomy is of paramount importance, due to the two way delay time in communications which makes impossible any cooperation form controllers located on the Earth, translating in a search for simple, computation limited, algorithms for guidance. At the same time, the need for confidence in the expected performances should be considered as a must, and leads to the request of robustness to unexpected variation of the environmental conditions, usually poorly known.

This paper aims to investigate the performances of different guidance strategies, aiming to produce a soft and accurate landing, which have a common requirement for simple sensors and actuators. The interest has been focused more on the evaluation of strategies performances in a real environment than on the introduction of novel guidance laws. Such a real environment is given by noise on the sensors' measurements and on an imprecise knowledge of the environment: these inaccuracies will be dealt with the help of estimators.

* Ph.D. student, Scuola di Ingegneria Aerospaziale, via Eudossiana 16 – 00184 Roma, Italy. AIAA Student Member.
‡ Associate Professor, Dipartimento di Ingegneria Aerospaziale e Astronautica, via Eudossiana 18 – 00184 Roma, Italy. AIAA Member.

Following the presentation by McInnes [1], a guidance to be used for comparison has been identified in the gravity turn, i.e. a strategy in which the thrust is directed opposite to the velocity vector: due to such a basic, constant requirement, the gravity turn is deemed as simple to implement. A simpler formulation of this strategy, useful for an open-loop control architecture, has been considered first; then, an approach allowing to provide a feedback of the current state and to use it for computing an error signal with respect to a previously defined descent profile has been adopted. Finally, a law derived from the addition of a potential function, using Lyapunov approach and obtained as an extension of the previous one, has been used to allow for precise landing possibly over an uneven terrain: in this case, the constraint on the thrust direction has been relaxed, and the thrust is no more parallel to the velocity, but allows for a better targeting of the designated touch down point.

In order to understand the performances while facing different environments, descents have been simulated both in the vacuum (Moon) as well as in thin (Mars) and thicker (Titan) atmospheres. In order to outline sensors' related concerns, two architectures, both of them deemed to respect the simplicity requirement, have been considered, namely a radio-altimeter, providing the altitude, and a radar Doppler measuring the slant range.

The paper should be intended as a preliminary effort carried out at the Università di Roma in order to gain a deeper knowledge on the better approaches for the entry phase in planetary exploration. The body of the paper is built as follows: a short remark on the estimators to be used in the analysis, completed by a relevant appendix, will be given first. The next step is the presentation of the three guidance strategies, which will be applied to the cases of the Moon, Mars and Titan. Various results are provided and analyzed, referring to both the architectures of the sensors' section and to the estimators adopted. Final remarks try to summarize the experience gained, and pave the way for further works. A short hint on the atmospheric models adopted for Mars and Titan are reported in the appendix. Following figure 1 offers a sketch of the problem and introduces the variables of interest.

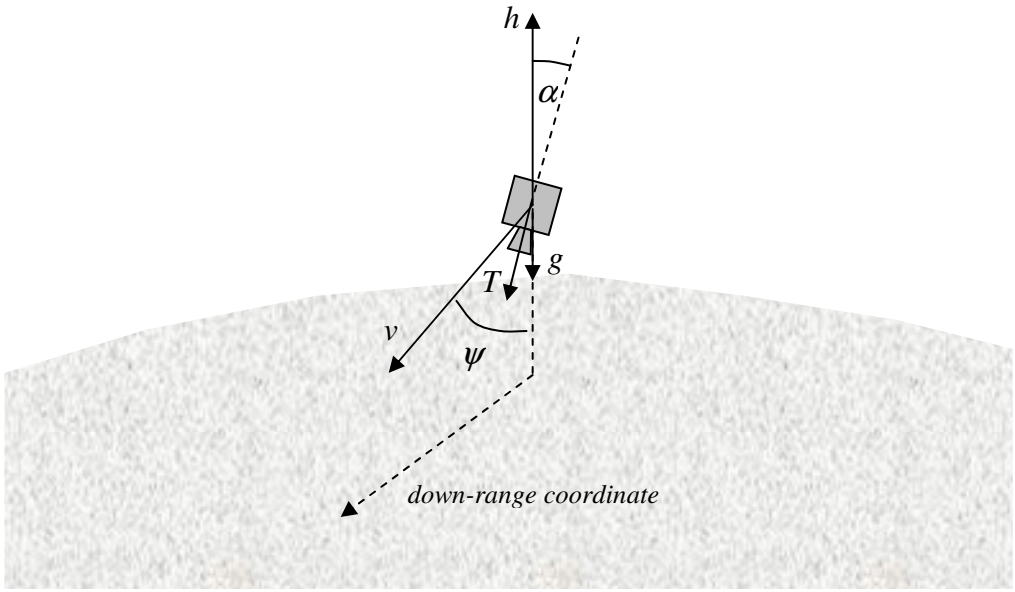

Figure 1. Geometry and variables in the terminal descent phase

II. Outline of the considered Estimators

The Kalman Filter [2], since its inception, proved to be a really useful tool due to its optimality for the linear systems subjected to a defined but widely accepted class of noises and for its recursive and computation limited formulation especially convenient for multiple input multiple output systems. In real world applications, the system and the measurement equations are not linear and a proper extension of the Kalman filter should be pursued. Such an extension is not a trivial issue, as the optimal solution theoretically calls for a complete description of the probability density function. The description be obtained only through the determination of a potentially never ending number of statistical parameters, and the resulting approximations generate sub-optimal solutions of the original problem.

The proposed approximations can be divided into four broad classes [3]: (1) analytical approximations, (2) numerical approximations, (3) Gaussian sum or multiple model filters and (4) sampling approaches. The first group includes the extended Kalman filter (EKF) which represents the strategy most widely used in the practical applications. This filter is based on the linearization of all non-linear models with respect to the current estimate, so that the traditional linear Kalman approach can be applied. The EKF presents two well-known drawbacks: a possible unstable behaviour if the assumptions of linearity between the updates intervals are locally violated and the derivation of the Jacobian matrices which is not an easy task in most applications. Instead the sampling approaches (4) approximate the density by a set of samples. Specifically, the unscented Kalman filter (UKF) uses a limited number of deterministically chosen samples and does not introduce the need to calculate the Jacobian, so avoiding the relevant EKF problem. This work will deals with these two methods (EKF and UKF) as alternative estimators for the kinematic state of the descending probe.

In order to better clarify the difference between the two estimators, let us consider that the application of the Kalman filter to nonlinear problems is a basically the attempt to estimate the statistics, and basically the first two centered moments, of a random variable subjected to nonlinear transformations. Following the approach by Julier and Uhlmann [4], suppose that $\vec{x}$ is a random variable with mean $\langle \vec{x} \rangle$ and covariance $\underline{\underline{P}}_{xx}$, and $\vec{y}$ a second random variable related to the first through a nonlinear function $\vec{f}$ representing the system dynamics:

$$\vec{y} = \vec{f}(\vec{x}) \tag{1}$$

The target is to determine the mean $\langle \vec{y} \rangle$ and the covariance ($\underline{\underline{P}}_{yy}$) of $\vec{y}$. Writing down the Taylor series (about $\vec{x}$) of $\vec{y}$:

$$\vec{y} = \vec{f}(\vec{x}) = \vec{f}\left[\langle \vec{x} \rangle + \vec{\delta x}\right] = \vec{f}\left[\langle \vec{x} \rangle\right] + \nabla \vec{f}\,\vec{\delta x} + \frac{1}{2}\nabla^2 \vec{f}\,\vec{\delta x}^2 + \frac{1}{3!}\nabla^3 \vec{f}\,\vec{\delta x}^3 + \frac{1}{4!}\nabla^4 \vec{f}\,\vec{\delta x}^4 + \ldots, \tag{2}$$

where $\vec{\delta x}$ is a Gaussian variable with zero mean and covariance $\underline{\underline{P}}_{xx}$, and $\nabla^n \vec{f}\,\vec{\delta x}^n$ is the *n*th order derivative term (with appropriate dimensions), it is possible to evaluate its mean and covariance:

$$\bar{\vec{y}} = \vec{f}\left[\bar{\vec{x}}\right] + \frac{1}{2}\nabla^2 \vec{f}\,\underline{\underline{P}}_{xx} + \frac{1}{4!}\nabla^4 \vec{f}\,E\left[\vec{\delta x}^4\right] + \ldots \tag{3}$$

$$\underline{\underline{P}}_{yy} = \nabla \vec{f}\,\underline{\underline{P}}_{xx}\left(\nabla \vec{f}\right)^T + \frac{1}{2\times 4!}\nabla^2 \vec{f}\left(E\left[\vec{\delta x}^4\right] - E\left[\vec{\delta x}^2\,\underline{\underline{P}}_{yy}\right] - E\left[\underline{\underline{P}}_{yy}\,\vec{\delta x}^2\right] + \underline{\underline{P}}_{yy}\right)\left(\nabla^2 \vec{f}\right)^T + \frac{1}{3!}\nabla^3 \vec{f}\,E\left[\vec{\delta x}^4\right]\left(\nabla \vec{f}\right)^T + \ldots \tag{4}$$

It can be seen from Eq. (3) that the mean is correctly computed up to an order which is equal to the one of the derivatives and moments included in its calculation, and similar considerations hold for the covariance [4]. Limiting to the more significant terms:

$$\begin{cases} \bar{\vec{y}} = \vec{f}\left[\langle \vec{x} \rangle\right] \\ \underline{\underline{P}}_{yy} = \nabla \vec{f}\,\underline{\underline{P}}_{xx}\left(\nabla \vec{f}\right)^T \end{cases}. \tag{5}$$

The EKF is based on the assumption that this local linearisation is a sufficient description of system nonlinearity, i.e. that second and higher order terms are negligible. The probabilistic density following the update is approximated by a Gaussian distribution and the mean and the covariance of this distribution are recursively calculated (by the Riccati equations). These equations, according to Eq. (5), will contain the Jacobian, evaluated at the last estimate of the state vector. More details and considerations about the EKF can be found in Appendix A.

The unscented transformation is an alternative method to compute the statistics of the random variable subjected to the nonlinear transformation. Without introducing Riccati equations, the Gaussian distribution assumed for the updated probabilistic density is computed by means of a set of purposely selected samples (the sigma points). The nonlinear transformation is actually computed at these point, and the mean and covariance ($\langle \vec{y} \rangle$ and $\underline{\underline{P}}_{yy}$) are there evaluated (see Appendix B for the equations). This (local) evaluation is correct up to the second order, i.e. one order

more than the EKF approach regarding the mean. A quite important operational detail of UKF is that mean and covariance are calculated only by means of standard vector and matrix operations, without including the Jacobian: it is therefore easy to implement for whichever process dynamics.

III. Gravity-Turn Descent

The interest on the gravity turn stems from the fact that such a guidance, in which the thrust vector is directed opposite to the vehicle velocity, is simple to implement and leads to a vertical descent immediately before the touchdown: this second consequence is extremely important to neglect any possible obstacle. The equation for the descent, assuming that the thrust is correctly directed opposite to the velocity (so that in Fig.1 $\alpha = \psi$) read as follows:

$$\begin{cases} \dot{v} = -ng + g\cos\psi \\ \dot{\psi} = -g\sin\psi / v \\ \dot{h} = -v\cos\psi \\ \dot{r} = v\cos\psi \end{cases} \tag{6}$$

This set allows to define a constant thrust to weight ratio leading to a successful descent, i.e. to a trajectory ending in a kinematic state with components [h=0, v=0]. However, as pointed out in Ref. 1, this approach requires a precise evaluation of the altitude at which the controlled descent should start, and to which the thrust amount depends on, as well as a correct implementation of the n provided by the thruster. Both these constraints actually make such an open-loop configuration unsuitable for accurate descents, especially if constraints on the touch-down location have to be introduced. It is however interesting to introduce the errors on these parameters, in order to have a hint on the solution that the open loop would provide in a real environment. Numerical simulations have been carried out for this gravity turn trajectory in the cases of the Moon, Mars and Titan, with an initial noise of the 1% on the altitude at which the manoeuvre begins. The sensor architecture considered is based on the altitude measurement only, provided as an example by a radio-altimeter, with a 1-σ error time varying and equal to 1% of the current altitude. Clearly, the down-range coordinate is not considered with this first approach, and no specific location could be targeted: in fact, even if the total time of the ideal descent can be a priori evaluated, and therefore the beginning of the manoeuvre selected accordingly, depending on the designed touch-down down-range, there is no way to counteract possible disturbances or misalignments.

Fig. 2 presents the altitude and vertical velocity curves for a descent on the Moon, showing good performances for the EKF. Fig. 3 investigates the filter behavior with an extremely rare measurement update, identifying the UKF as the best choice. Such a hint is better clarified, for a range of update rates, in Fig. 4, while Fig. 5 compares the two filters with respect to the standard deviation of the sensor measurement (altitude). It appears as the two filters are almost equivalent when new measurements are available very often; as a latency begins, the UKF is clearly superior.

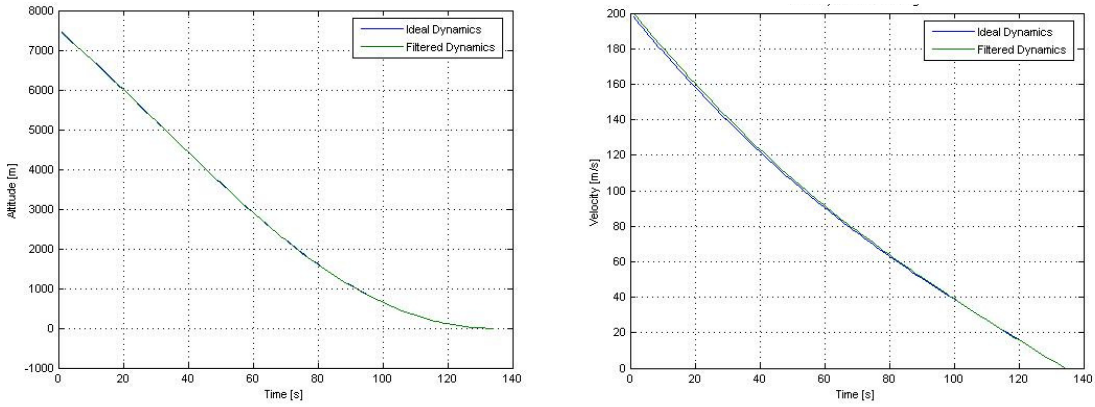

Figure 2. Time history of the altitude and of the velocity for a gravity turn descent on the Moon

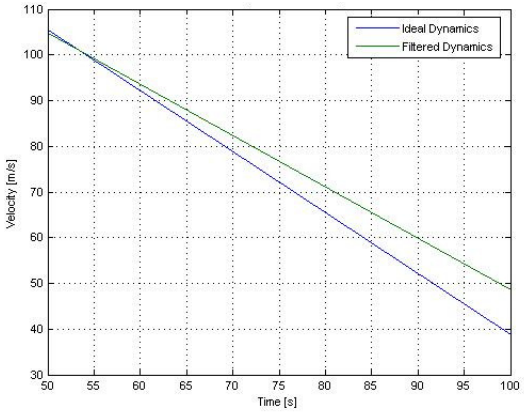

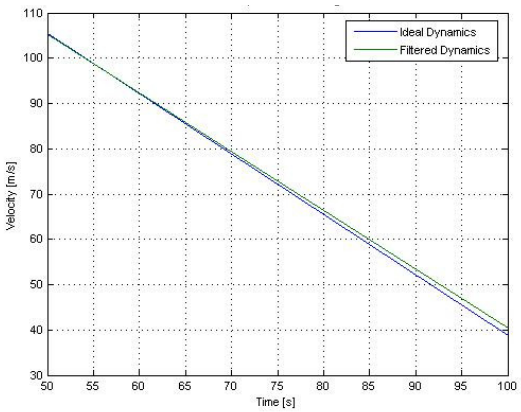

Figure 3. Lunar descent - A comparison between the estimators (EKF left – UKF right)

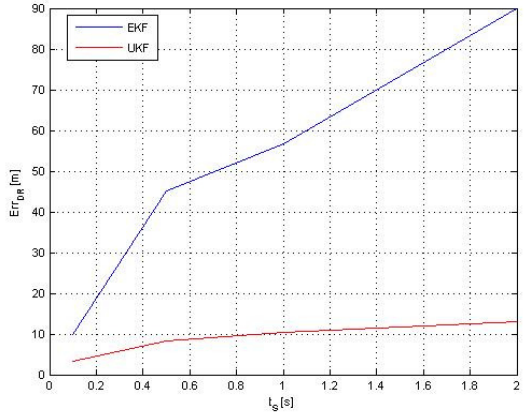

Figure 4. Comparison between EKF and UKF different sampling time (Moon case)

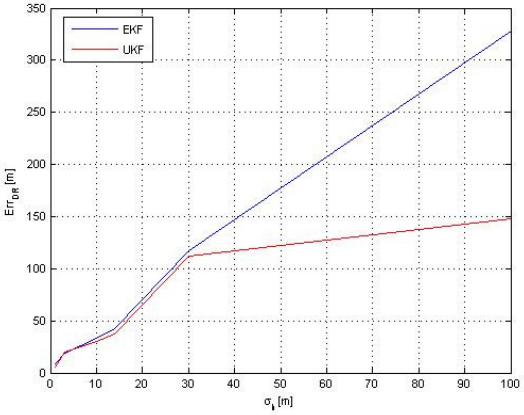

Figure 5. Comparison between EKFand UKF for different sensor errors (Moon case)

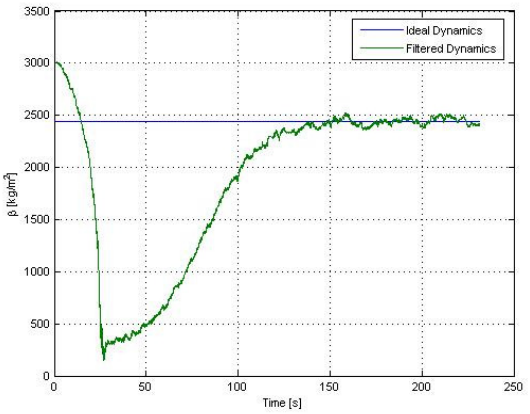

Figure 6. Mars descent – estimate of the ballistic coefficient

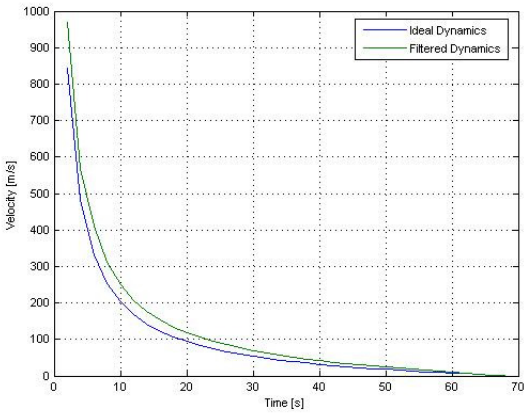

Figure 7. Velocity profile for a descent on Titan

Following figures refer to the two cases of descent into atmosphere. Figure 6 shows the estimate of the ballistic coefficient in the Martian case: it has to be remarked that the only measurement available relates to the altitude, so that no direct information on velocity, and therefore on drag, is available. Figure 7 refers to the descent on Titan, with a velocity profile that, due to the atmosphere, is clearly different - steepest at the beginning, then softer as the probe approaches the ground - with respect to the case of the Moon, where deceleration was almost constant (Fig. 2).

IV. Path-Shaping Descent

A slightly more complicated representation can be used in order to take into account possible inaccuracies, but it does necessarily imply the possibility to change the thrust level. The approach proposed by McInnes [1] included an exponential profile for the velocity as function of the altitude:

$$\tilde{v}(h) = v_o\left(1 - e^{-\lambda h}\right) \tag{7}$$

which allows to select the descent trajectory in a set defined by λ parameter, and enables to feedback a correction signal equal to

$$u = v - \tilde{v}(h) \tag{8}$$

To combine Eq. (6) and Eq. (8), imposing:

$$\dot{u} = -ku \tag{9}$$

results in the following thrust to weight ratio, variable with the height

$$\tilde{n} = \left(1 - \frac{v}{g}\frac{\partial v}{\partial h}\right)\cos\psi + \frac{k}{g}\left(v - \tilde{v}(h)\right) \tag{10}$$

The thrust is still parallel to the velocity vector as in the previous case, but the designer has the degree of freedom to select the velocity profile. From the control-oriented point of view, the architecture is now closed loop, and the filtering of the disturbances entering through the sensor becomes a key factor. Both the EKF and UKF have been tried, and both of them proved successful (for the Moon, Mars and Titan) in estimating the altitude and provide the correct error signal to the controller. The case reported in Fig. 8, other than showing the obtained velocity profile, completely different from the one given by the previous, open loop case, recalls the difference between EKF and UKF once the update rate decreases (in the figure, sampling time is 0.1s, definitely not a slow value, even compared to Fig. 4). The problem is clearly enhanced by the feedback, and in fact a 100 times higher update should be needed for EKF to match the plotted behaviour of UKF, posing a difficult requirement to the system.

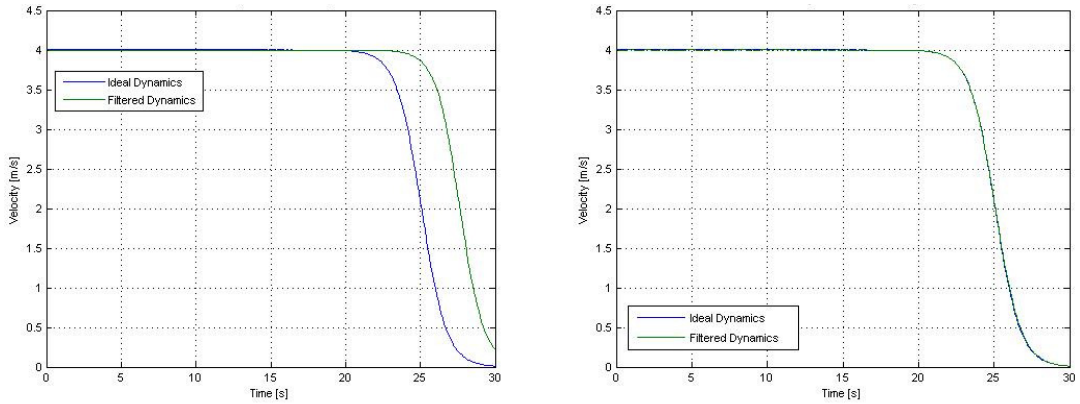

Figure 8. Comparison between the estimators in a Moon descent with a path shaping guidance (EKF left – UKF right)

V. Precision Descent

The gravity turn descent depicted in the previous paragraph allows to a soft landing but does not include any requirement on the landing location, i.e., any constraint on the downrange distance run from the entry point till the touch down point. Requirement for landing in a pre-assigned location is however of paramount importance, and a chance to take it into account is given by the potential function guidance. The idea proposed in Ref. 1 is to impose a profile, which will be given by means of an autonomous potential function

$$\phi(\vec{x}) = (\vec{x} - \vec{x}_{td})^T M (\vec{x} - \vec{x}_{td}) + V \tag{11}$$

in which $\vec{x}_{td}$ is the designated touch down point, M is the matrix associated with the quadratic form and allows to tailor the descent, while V (still appositional function, not depending on time) could take into account the orography of the site or some operational constraint.

The velocity will be obtained as the product of a desired descent profile times the gradient of the potential function [1]

$$\vec{v} = -\tilde{v}(h) \frac{\nabla\phi}{\|\nabla\phi\|} \tag{12}$$

where $\tilde{v}(h)$ is the desired velocity profile with respect to the altitude given by Eq. (7). As the purposely introduced potential function ϕ satisfies the rules assessed by Lyapunov's theory, the touch down point results globally attractive, or, in other words, the descent will smoothly proceed in a stable manner. The acceleration needed can be evaluated by means of

$$\dot{\vec{v}} = \left\{ \frac{\partial \vec{v}}{\partial \vec{x}} \right\}_{3\times 3} \cdot \vec{v} \tag{13}$$

(in the simulation, the matrix has been symbolically evaluated in Matlab (The Mathworks, Inc.), and an analytic form, useful for guidance, results), and the per mass thrust – this time not necessarily opposite to the velocity - can be finally evaluated (figure 9), with only a gravity model to be stored on board, for the Moon, and with a model for the drag forces also for the planets with atmosphere, following

$$\vec{T} = \dot{\vec{v}} - \vec{g} - \vec{f}_{drag} \tag{14}$$

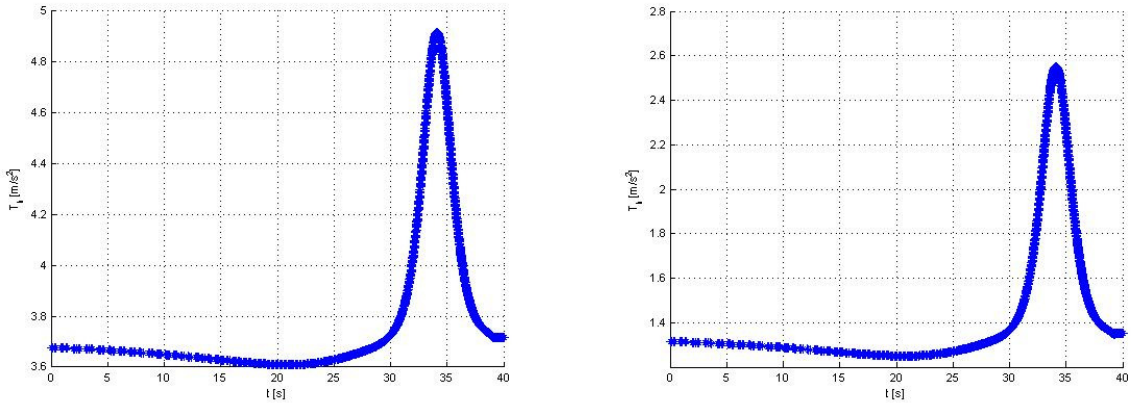

Figure 9. Thrust vertical component for Mars (left) and Titan (right) descent

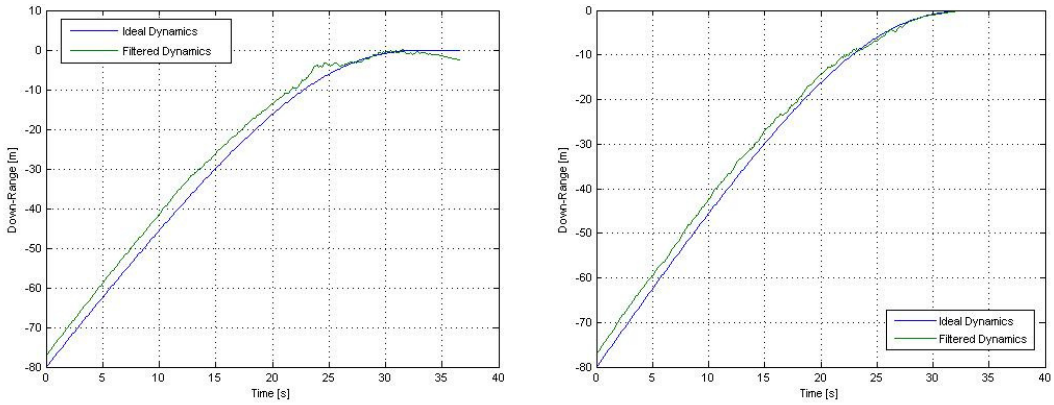

Figure 10. Lunar descent - Down range coordinate estimates vs. time obtained with two different kind of measurements: altitude (left) and slant range (right)

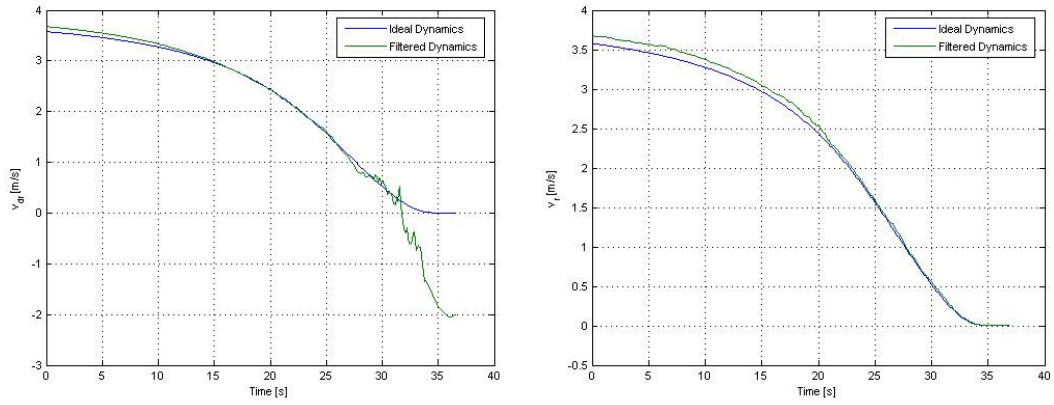

Figure 11. Differences in the horizontal velocity estimation between the two sensors' architectures (Moon)

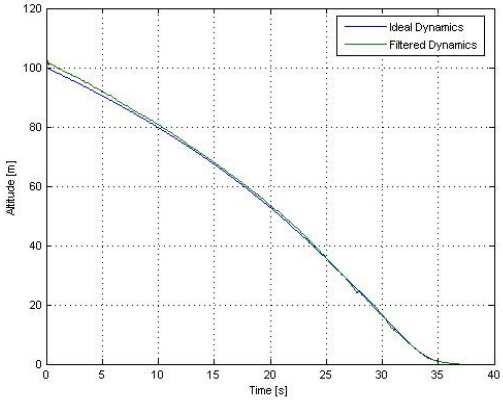

Figure 12. Descent over Mars – Estimate of the altitude profile with 2% noise on density and initial altitude error

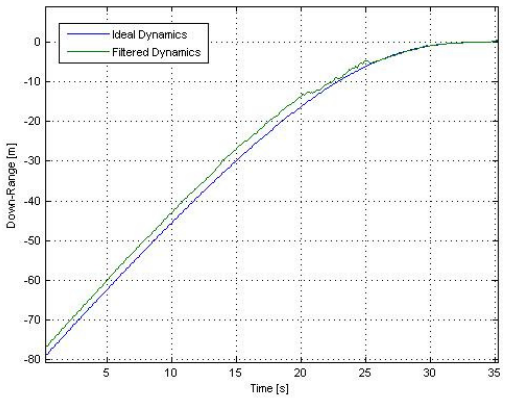

Figure 13. Descent over Titan – Down range estimate with 10% noise on the atmospheric density and initial altitude error

Again, we are interested in evaluating the performances of this approach while inaccuracies in the state determination are present. With respect to the previous cases, the down-range coordinate could be referred to a well defined, previously known point ($\vec{x}_{td}$ in Eq. (11)). In order to deeper exploit this option, a sensor other than the radio altimeter has been also considered, introducing the slant range measurement: of course, as clearly shown in Figure 10, such a choice translates in better results for the downrange, due to the easier observability of this parameter. The difference becomes larger when looking at the horizontal velocity: the altitude measurements fail to recover this variable, while the slant-range ones succeed, even if the operationally simple addition of the range rate has not be done, as in the case plotted in Fig. 11. This sensor architecture is beneficial also for atmospheric descents where, allowing for a better estimates of the velocity and therefore of the drag effect, is capable to correctly handle significant process noise, as shown in Fig. 12 for Mars and in Fig. 13 for Titan.

VI. Conclusion

The evaluation of the robustness of solar system bodies descending trajectories based on a simple gravity turn, with a thrust parallel to the velocity vector, on its extension allowing to shape the velocity profile and (at the cost of the thrust no more parallel to the velocity) the altitude profile, has been presented. Sensors' architectures have been kept purposely simple, with only altitude or slant range data available. Both the cases of a descent in the vacuum (Moon) and of the entry in an atmosphere (thinner as Mars, or thicker as Titan) have been numerically simulated. The robustness has been tested with respect to inaccuracies in the initial state of the terminal descent, to the noise level on the measurements, and to the mismodeling of the environment (for atmospheric descent). Two different estimators derived from Kalman approach have been evaluated, namely the EKF and the UKF.

Results show the capability of the filters to supply measurements such that control loop achieve the targets. UKF proved to be superior with respect to input latency problem, meaning that is able to provide the same result of the EKF even if the measurement update rate is at least one order of magnitude lower. Future additional studies will consider a different estimator, the Particle Filter, deemed to perform quite well even with strong inaccuracies on the process: however the computational burden required limits its interest for simple probes as the ones targeted with this work. With respect to sensors' architectures, the slant range observable provided, as expected, better performances than the altitude, even if no range rate was considered. The advantage is especially true while descending into an atmosphere and with the guidance allowing to point at a specific touch down point, as the slant range obviously provides better insight of the components parallel to the ground, as the downrange and the horizontal velocity.

Appendix

A. Extended Kalman Filter (EKF) [2,4]

The EKF is applied at nonlinear systems subject to an additive noise:

$$\vec{x}_k = \vec{f}(\vec{x}_{k-1}) + \vec{v}_{k-1} \tag{A.1}$$

$$\vec{z}_k = \vec{h}(\vec{x}_k) + \vec{w}_k \tag{A.2}$$

where $\vec{x}_k$ is a (n-dimensional) vector representing the system state at time k, $\vec{v}_k$ the process noise vector related to the model errors and unknown external disturbances, $\vec{z}_k$ the observations vector (altitude or slant-range measurements) and $\vec{w}_k$ the measurement noise. Noise is zero mean and, indicating different time with i,j, the following assumptions hold:

$$E\left[\vec{v}_i\ \vec{v}_j^T\right] = \delta_{ij}\underline{\underline{Q}}_i, \quad E\left[\vec{w}_i\ \vec{w}_j^T\right] = \delta_{ij}\underline{\underline{R}}_i, \quad E\left[\vec{v}_i\ \vec{w}_j^T\right] = 0, \quad \forall i, j. \tag{A.3}$$

The Kalman filter propagates recursively the first two moments associated with the state following a characteristic structure "prediction-update". $\vec{f}$ and $\vec{h}$ are approximated by:

$$\begin{cases} \underline{\underline{F}} = \left.\dfrac{\partial \vec{f}(\vec{x})}{\partial \vec{x}}\right|_{\vec{x}=\hat{\vec{x}}} \\ \underline{\underline{H}} = \left.\dfrac{\partial \vec{h}(\vec{x})}{\partial \vec{x}}\right|_{\vec{x}=\hat{\vec{x}}} \end{cases} \tag{A.4}$$

while the fundamental matrix ($\underline{\underline{\Phi}}$, depending on the $\underline{\underline{F}}$ and relating $\vec{x}_{k-1}$ to $\vec{x}_k$), is usually approximated with the first two terms of the Taylor expansion series of $e^{\underline{\underline{FT_s}}}$:

$$\underline{\underline{\Phi}}_k \approx I + \underline{\underline{F}} T_s \tag{A.5}$$

where I is a identity matrix and T_s the sampling time. The Riccati equations [2] can be written as:

$$\begin{cases} \underline{\underline{P}}_k^- = \underline{\underline{\Phi}}_k \underline{\underline{P}}_{k-1} \underline{\underline{\Phi}}_k^T + \underline{\underline{Q}}_k \\ \underline{\underline{K}}_k = \underline{\underline{P}}_k^- \underline{\underline{H}}^T \left[\underline{\underline{H}}\, \underline{\underline{P}}_k^- \underline{\underline{H}}^T + \underline{\underline{R}}_k \right]^{-1} \\ \underline{\underline{P}}_k = \left[I - \underline{\underline{K}}_k \underline{\underline{H}} \right] \underline{\underline{P}}_k^- \end{cases}, \tag{A.6}$$

with $\underline{\underline{P}}_k^-$ the value of state estimation error covariance matrix before the update and $\underline{\underline{P}}_k$ its updated value. The state estimation is an optimal blending with a gain ($\underline{\underline{K}}_k$) of an *a-priori* state estimation ($\hat{\vec{x}}_k^-$) and the difference between the real ($\vec{z}_k$) and the predicted measurement ($\vec{h}(\hat{\vec{x}}_k^-)$):

$$\hat{\vec{x}}_k = \hat{\vec{x}}_k^- + \underline{\underline{K}}_k (\vec{z}_k - \vec{h}(\hat{\vec{x}}_k^-)) . \tag{A.7}$$

B. Unscented Kalman Filter (UKF) [4, 6]

Given the last estimate of state vector, $\hat{\vec{x}}_{k-1}$, the real (n-dimensional) variable $\vec{x}$ can be approximated by a finite number of weighted points opportunely selected. These points are then stored in the columns of the $n \times (2n+1)$ matrix $\underline{\underline{\chi}}_{k-1}$:

$$\begin{cases} (\underline{\underline{\chi}}_{k-1})_0 = \hat{\vec{x}}_{k-1} \\ (\underline{\underline{\chi}}_{k-1})_i = \hat{\vec{x}}_{k-1} + \left(\sqrt{(n+\lambda)\underline{\underline{P}}_{k-1}} \right)_i, \quad i = 1, \ldots, n \\ (\underline{\underline{\chi}}_{k-1})_{i+n} = \hat{\vec{x}}_{k-1} - \left(\sqrt{(n+\lambda)\underline{\underline{P}}_{k-1}} \right)_i, \quad i = n+1, \ldots, 2n \end{cases}, \tag{B.1}$$

where[§] $\lambda \in \Re$, $n \in Z$ and $\left(\sqrt{(n+\lambda)\underline{\underline{P}}_{xx}} \right)_i$ is the ith column in the root squared and symmetric matrix $(n+\lambda)\underline{\underline{P}}_{xx}$. As the EKF, also the UKF presents the recursive scheme "prediction-update". In the UKF, the prediction step starts with the propagation of each set of sigma points (given by the columns of $\underline{\underline{\chi}}_{k-1}$) through the Δt time interval:

[§] n and λ are tuning term related [3] to the higher order term considered in the Taylor series (4) and (5).

$$\left(\underline{\underline{\chi}}_k\right)_i = \vec{f}\left(\left(\underline{\underline{\chi}}_{k-1}\right)_i\right), \quad i = 0,\ldots,2n \tag{B.2}$$

where $\vec{f}$ is always the dynamics considered. By means of (B.2) it is possible to write the *a-priori* state estimation as a weighted sum:

$$\hat{\vec{x}}_k^- = \sum_{i=0}^{2n} W_i^{(m)} \left(\underline{\underline{\chi}}_k\right)_i , \tag{B.3}$$

$$\begin{cases} W_0^{(m)} = \dfrac{\lambda}{(n+\lambda)} \\ W_i^{(m)} = \dfrac{1}{2(n+\lambda)}, \quad i = 1,\ldots,2n \end{cases} . \tag{B.4}$$

The *a-priori* error estimation covariance matrix is given by:

$$\underline{\underline{P}}_k^- = \sum_{i=0}^{2n} W_i^{(c)} \left[\left(\underline{\underline{\chi}}_k\right)_i - \hat{\vec{x}}_k^-\right]\left[\left(\underline{\underline{\chi}}_k\right)_i - \hat{\vec{x}}_k^-\right]^T + \underline{\underline{Q}}_k , \tag{B.5}$$

with $\underline{\underline{Q}}_k$ that is the process error covariance matrix, already defined in (A.3), and:

$$\begin{cases} W_0^{(c)} = \dfrac{\lambda}{(n+\lambda)} + \left(1 - \alpha^2 + \beta\right) \\ W_i^{(c)} = \dfrac{1}{2(n+\lambda)}, \quad i = 0,\ldots,2n \end{cases} . \tag{B.6}$$

(α is a parameter related to the spread of sigma points, while β takes into account initial knowledge about $\vec{x}$ distribution).

To carry out the correction step the columns of $\underline{\underline{\chi}}_{k-1}$ are transformed by the measurement function $\vec{h}$:

$$\left(\underline{\underline{\gamma}}_k\right)_i = \vec{h}\left(\left(\underline{\underline{\chi}}_k\right)_i\right), \quad i = 0,\ldots,2n , \tag{B.7}$$

to obtain the measurement prediction:

$$\hat{\vec{z}}_k^- = \sum_{i=0}^{2n} W_i^{(m)} \left(\underline{\underline{\gamma}}_k\right)_i . \tag{B.8}$$

At this point it is possible to update the state estimation:

$$\hat{\hat{x}}_k = \hat{\hat{x}}_k^- + \underline{\underline{K}}_k \left(\vec{z}_k - \hat{\hat{z}}_k^- \right). \tag{B.9}$$

with the Kalman gain matrix computed by:

$$\underline{\underline{K}}_k = \underline{\underline{P}}_{\hat{\hat{x}}_k \hat{\hat{z}}_k} \underline{\underline{P}}^{-1}_{\hat{\hat{z}}_k \hat{\hat{z}}_k} \tag{B.10}$$

where

$$\underline{\underline{P}}_{\hat{\hat{z}}_k \hat{\hat{z}}_k} = \sum_{i=0}^{2n} W_i^{(c)} \left[(\mathcal{Y}_k)_i - \hat{\hat{z}}_k^- \right] \left[(\mathcal{Y}_k)_i - \hat{\hat{z}}_k^- \right]^T + \underline{\underline{R}}_k \tag{B.11}$$

and

$$\underline{\underline{P}}_{\hat{\hat{x}}_k \hat{\hat{z}}_k} = \sum_{i=0}^{2n} W_i^{(c)} \left[(\underline{\underline{\chi}}_k)_i - \hat{\hat{x}}_k^- \right] \left[(\mathcal{Y}_k)_i - \hat{\hat{z}}_k^- \right]^T . \tag{B.12}$$

where $\underline{\underline{R}}_k$ is the measurement noise matrix already defined in (Eq. A.3). The last update step deals with the *a-posteriori* error covariance:

$$\underline{\underline{P}}_k = \underline{\underline{P}}_k^- - \underline{\underline{K}}_k \underline{\underline{P}}_{\hat{\hat{z}}_k \hat{\hat{z}}_k} \underline{\underline{K}}_k^T \tag{B.13}$$

C. Mars atmospheric model

The model used in this work has been introduced by Sirinian [6], and is based on the hypothesis of a temperature which is linearly decreasing with the height up to 60 km, as

$$T(h) = T_o - 1.4167 \cdot h \tag{C.1}$$

Introducing the relations for the hydrostatic equilibria and the gas law,

$$dp = -\rho g \, dz \qquad p = \rho R T \tag{C.2}$$

and considering the CO_2 only , which by the way sums up to 95% in weight of the Martian atmosphere, it is possible to find the relation for the pressure and the density as function of the altitude:

$$p = k_1 p_o \left(\frac{158 \cdot h}{3385 + h} \right)^{12.5} e^{-\frac{44200}{3385+h}} \tag{C.3}$$

$$\rho(h) = k_2 \frac{p(h)}{T(h)} \tag{C.4}$$

where $k_1 = 78\times10^3$ and $k_2 = 5.2\times10^{-3}$ are the constant to have the variables in MKS units. T_o and p_o have been captured from the measurement campaign performed during NASA Pathfinder mission.

D. Titan atmospheric model

As far as it concerns the atmosphere of Titan, a classical exponential profile, deriving from an isothermal assumption, has been used (note that this approximation could be accepted due to the limited range of interest in altitude). The values for the scale height and the density at the ground have been selected according to Ref. 7.

References

[1] McInnes, C.R., "Path Shaping Guidance for Terminal Lunar Descent", *Acta Astronautica*, Vol. 36, No. 7, 1995, pp. 367-377.

[2] Zarchan, P. and Musoff, H., *Fundamental of Kalman Filtering*, Progress in Astronautics and Aeronautics, Vol. 190, AIAA, Washington, DC, 2000.

[3] Ristic, B., Arumpalam, S., Gordon, N., *Beyond the Kalman Filter*, Artech House, Boston, 2004.

[4] Julier, S.J., Uhlmann, J.K. and Durrant-Whyte, H.F. "A New Approach for Filtering Nonlinear Systems", *Proceedings of the American Control Conference,* Seattle (WA)*,* 1995, pp. 1628-1632.

[5] Zarchan, P., *Tactical and Strategic Missile Guidance*, 4th ed., Progress in Astronautics and Aeronautics, AIAA, Washington, DC, 2002.

[6] LaViola, J.J.Jr. "A Comparison of Unscented and Extended Kalman Filtering for Estimating Quaternion Motion", *Proceedings of the American Control Conference*, vol.3, 2003, pp. 2435-2440.

[7] Sirinian, M.D., "Il volo su Marte", Scuola Ingegneria Aerospaziale IOR_20, Univ. Roma La Sapienza, Roma, Italy, 1980.

[8] URL: http://www.esa.int/SPECIALS/Cassini-Huygens/SEMU76HHZTD_0.html [cited 10 August 2007].